



저작자표시-비영리-변경금지 2.0 대한민국

이용자는 아래의 조건을 따르는 경우에 한하여 자유롭게

- 이 저작물을 복제, 배포, 전송, 전시, 공연 및 방송할 수 있습니다.

다음과 같은 조건을 따라야 합니다:



저작자표시. 귀하는 원 저작자를 표시하여야 합니다.



비영리. 귀하는 이 저작물을 영리 목적으로 이용할 수 없습니다.



변경금지. 귀하는 이 저작물을 개작, 변형 또는 가공할 수 없습니다.

- 귀하는, 이 저작물의 재이용이나 배포의 경우, 이 저작물에 적용된 이용허락조건을 명확하게 나타내어야 합니다.
- 저작권자로부터 별도의 허가를 받으면 이러한 조건들은 적용되지 않습니다.

저작권법에 따른 이용자의 권리와 책임은 위의 내용에 의하여 영향을 받지 않습니다.

이것은 [이용허락규약\(Legal Code\)](#)을 이해하기 쉽게 요약한 것입니다.

[Disclaimer](#)



Dimensional Stability of Implant Surgical Guides: Effects of Thickness, Arch Type, and Storage Period

Kim, KyungHwan

**Department of Dentistry
Graduate School
Yonsei University**

Dimensional Stability of Implant Surgical Guides: Effects of Thickness, Arch Type, and Storage Period

Advisor Kim, Jong-Eun

**A Master's Thesis Submitted
to the Department of Dentistry
and the Committee on Graduate School
of Yonsei University in Partial Fulfillment of the
Requirements for the Degree of
Master of Dental Science**

Kim, KyungHwan

June 2025

**Dimensional Stability of Implant Surgical Guides: Effects of Thickness,
Arch Type, and Storage Period**

**This Certifies that the Master's Thesis
of Kim, KyungHwan is Approved**

Committee Chair **Lee, Hyeonjong**

Committee Member **Kim, Jaeyoung**

Committee Member **Kim, Jong-Eun**

**Department of Dentistry
Graduate School
Yonsei University
June 2025**

TABLE OF CONTENTS

| | |
|--|-----|
| LIST OF FIGURES | ii |
| LIST OF TABLES..... | iii |
| ABSTRACT IN ENGLISH | iv |
| 1. INTRODUCTION..... | 1 |
| 2. MATERIALS AND METHODS | 3 |
| 2.1. Study Design and Experimental Groups | 3 |
| 2.2. CAD Design of Surgical Guides | 4 |
| 2.3. 3D Printing Protocol..... | 5 |
| 2.4. Storage Conditions and Measurement Schedule | 8 |
| 2.5. Dimensional Analysis and Scanning Protocol | 8 |
| 2.6. Seating Accuracy Analysis | 8 |
| 2.7. Statistical Analysis..... | 9 |
| 3. RESULTS | 10 |
| 3.1. Dimensional Stability (RMSE Results) | 10 |
| 3.2. Color Map Analysis of Deformation Patterns | 13 |
| 3.3. 3D Printing Protocol..... | 16 |
| 4. DISCUSSION | 19 |
| 5. CONCLUSION | 23 |
| REFERENCES | 24 |
| ABSTRACT IN KOREAN | 30 |

LIST OF FIGURES

<Fig 1> Flowchart of study design

<Fig 2> Thickness measured from the outer contour of the guide body, excluding the sleeve

- (A) Cross-sectional view illustrating the reference area for thickness measurement in the FA surgical guide design
- (B) Cross-sectional view illustrating the reference area for thickness measurement in the PA surgical guide design

<Fig 3> Cross-sectional measurement of sleeve wall thickness (3.02 mm) in the surgical guide design

<Fig 4> Printing orientation of surgical guides at a 180° angle relative to the build platform

<Fig 5> Partial-arch surgical template

<Fig 6> Full-arch surgical template

<Fig 7> Time-dependent changes in RMSE across different guide thicknesses under the partial-arch design

<Fig 8> Time-dependent changes in RMSE across different guide thicknesses under the full-arch design

<Fig 9> Colormap of dimensional deviation in 3D-printed surgical guides

<Fig 10> Workflow of colormap segmentation and area extraction

<Fig 11> Time-dependent changes in red and blue area ratios extracted from colormaps for different surgical guide designs and thicknesses. Blue and red regions represent deviations below -0.05 mm and above $+0.05$ mm, respectively

<Fig 12> Time-dependent changes in seating accuracy across different guide thicknesses under the partial-arch design

<Fig 13> Time-dependent changes in seating accuracy across different guide thicknesses under the full-arch design

<Fig 14> Colormap of dimensional deviation in 3D-printed surgical guides when seating on a dental model cast



LIST OF TABLES

<Table 1> Root mean square error values of 3D-printed surgical guides with partial arch over 14 days

<Table 2> Root mean square error values of 3D-printed surgical guides with full arch over 14 days

<Table 3> Seating accuracy of 3D-printed surgical guides with partial-arch design over 14 days

<Table 4> Seating accuracy of 3D-printed surgical guides with full-arch design over 14 days

ABSTRACT

Dimensional Stability of Implant Surgical Guides: Effects of Thickness, Arch Type, and Storage Period

Purpose: This study aimed to investigate the effects of guide thickness, arch span, and storage duration on the dimensional stability and seating accuracy of three-dimensional (3D)-printed implant surgical guides.

Materials and Methods: Stereolithography (SLA) in partial-arch (PA) and full-arch (FA) designs with three thickness levels (2, 3, and 4 mm) was used to develop 48 surgical guides. The guides were stored for up to 14 days and assessed at five time points (0, 1, 3, 7, and 14 days). Dimensional changes were quantified based on root mean square error (RMSE) and visualized through colormap analysis. Seating accuracy was assessed using model-based mounting analysis.

Results: Most dimensional deformation occurred from days 0 and 1, with stabilization observed thereafter. In the PA group, 2-mm-thick guides demonstrated a marked increase in deformation on day 7 (RMSE: $200.14 \pm 37.52 \mu\text{m}$), indicating a vulnerability in thinner designs. In contrast, 3-mm and 4-mm PA guides maintained relatively stable RMSE levels over time (e.g., 4 mm: $45.90 \pm 3.73 \mu\text{m}$ on 14 days), demonstrating improved dimensional stability. FA guides exhibited lower overall RMSE values compared with PA guides (e.g., FA of 4 mm: $65.16 \pm 0.47 \mu\text{m}$ on 14 days), along with consistent seating accuracy throughout the study period. Three-way analysis of variance confirmed significant effects and interactions among thickness, arch span, and storage duration on both deformation and seating accuracy ($p < 0.001$).

Conclusions: The results indicate that increasing surgical guide thickness improves dimensional stability and reduces deformation. A minimum thickness of 3 mm is recommended, with 4 mm being preferred in PA designs. An adequate post-curing stabilization period is essential to ensure clinical accuracy in implant placement.

Key words: Implant surgical guide; Guide thickness; Dimensional stability; Arch span; Storage duration; Seating accuracy; Root mean square error; 3D printing

1. INTRODUCTION

Digital dentistry has undergone considerable advancements, resulting in increased application of three-dimensional (3D) printing technology in developing implant surgical guides (1–3). This technology provides high precision and manufacturing efficiency, which improves accuracy and predictability throughout the process from surgical planning to clinical application, especially when combined with digital workflows (1, 4, 5). These guides facilitate precise design and customized fabrication, thereby improving accuracy (6, 7) and efficiency (8, 9) in implant surgery. Surgical guides play a crucial role in improving treatment outcomes by averting damage to critical anatomical structures, such as nerves and blood vessels (10, 11). Further, they help maintain the implant's correct position, which ensures improved surgical success rates (12, 13). Considering that implant surgery performed with surgical guides is a flapless surgical procedure, in which the implants are placed through small incisions created in the gingiva without direct alveolar bone access, the guides must demonstrate a high degree of accuracy. Consequently, several studies have been conducted to assess the precision and accuracy of surgical guides. Various factors still compromise its accuracy, including the data registration process, the design of the guide, the surgical procedure, and dimensional changes in the material, despite the widespread adoption of guided implant surgery (14).

The widely applied 3D printing technologies employed in dentistry currently comprise stereolithography (SLA), digital light processing (DLP), and fused deposition modeling (FDM) (15–17). Each technology possesses distinct advantages and applications, contributing to improving efficiency and precision in dental treatment. These technologies are frequently used to develop dental prostheses, surgical guides, and orthodontic appliances (1, 18). FDM technology, in particular, has found primary application in fabricating dental models for educational purposes. This technology is distinguished by its cost-effectiveness, ease of processing, and the ability to generate functional parts with minimal post-processing (19). However, FDM technology exhibits certain limitations, including relatively low precision and rough surfaces, which hinder its application in the production of high-precision dentistry devices required in clinical settings (19, 20). Conversely, SLA and DLP technologies demonstrate superior accuracy, particularly in dental applications where high precision is paramount, such as establishing implant surgical guides (21, 22). Further, SLA and DLP provide sufficient accuracy to produce precise structures such as full-arch (FA) models (21, 22). Both techniques have been documented to improve accuracy with reduced guide sizes (4). DLP has exhibited superior accuracy compared with SLA (4, 23); however, SLA is acknowledged to demonstrate greater durability under particular conditions (24). Therefore, the selection of a given technique should be identified by the intended application, considering the required accuracy and durability level.

Both SLA and DLP technologies, using photopolymerized resins, have been susceptible to dimensional deviations during fabrication, post-processing, and storage conditions (25). These dimensional variations can induce structural distortion of the surgical guide, which adversely affects the accuracy of implant surgery and, consequently, the clinical outcomes (26). Furthermore, studies

have revealed the potential for 3D-printed surgical guides to undergo additional physical deformation over time caused by variables such as material composition and storage conditions (27–29). To date, studies have primarily focused on the effects of material type, printing technique, and printing orientation on dimensional stability (27, 30, 31). However, studies that have systematically and simultaneously analyzed the effects of thickness variation and storage duration on surgical guide deformation remain limited. Of particular concern is the paucity of studies that have systematically and simultaneously compared partial-arch (PA) and FA designs to assess the effects of structural differences on deformability.

The advent of computer-assisted surgery technology has guided the development of both static and dynamic approaches in the domain of implant surgery (28). Static approaches employ prefabricated surgical guides to position implants in predetermined locations, with the physical accuracy of these guides exerting a substantial effect on outcomes (32). Conversely, dynamic methods employ a real-time navigation system that enables continuous implant position adjustment during the surgical procedure. The impact of the guide thickness in these two methods can vary, especially in static methods, where the precise guide fabrication and its dimensional stability are more crucial (33). However, the impact of guide thickness variation on dimensional stability and deformability still warrants thorough investigation. In particular, studies that have systematically analyzed the deformation behavior during storage over a specific period are limited.

This study aimed to compare and analyze deformation patterns over time in FA and PA surgical guides fabricated using SLA-based 3D printing. Specifically, this research aimed to identify the effects of guide thickness on deformability and assess how increased storage duration affects dimensional stability across different thicknesses. Further, the study systematically compared PA and FA designs to determine structural effects on deformability and dimensional stability.

Ultimately, this investigation aimed to establish optimal thickness guidelines and provide clinical recommendations concerning the most appropriate timing for surgical guide application, thereby improving the accuracy of implant placement. Furthermore, the study assessed the dimensional stability and seating accuracy of the fabricated surgical guides through precise mounting analysis. The null hypothesis was that variations in guide thickness, arch span length, and storage duration would exhibit no significant effect on deformation and seating accuracy.

2. MATERIALS AND METHODS

2.1. Study Design and Experimental Groups

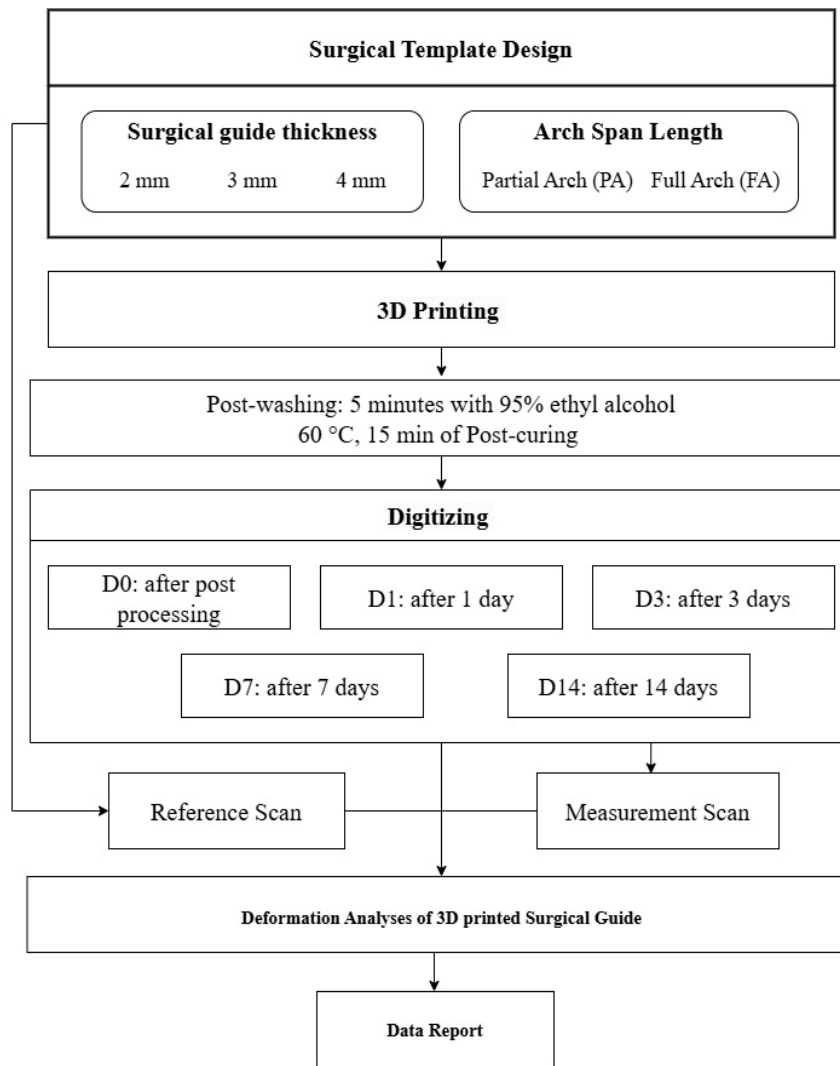


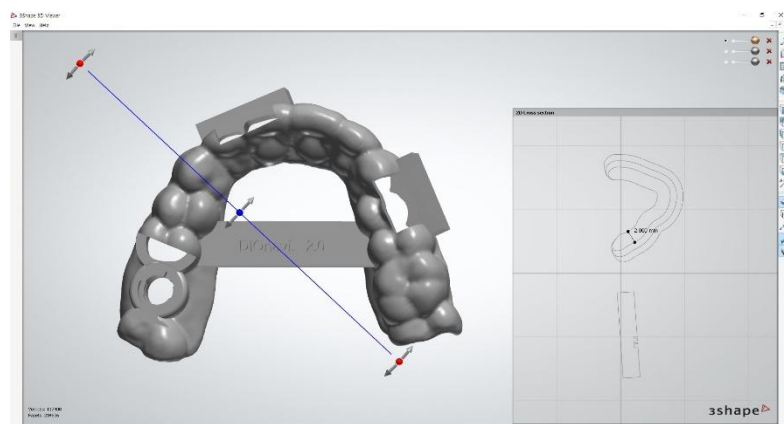
Fig. 1. Flowchart of study design

Figure 1 illustrates the study design in the flowchart. The present study was designed as an *in vitro* experiment aimed at assessing the dimensional stability and deformability of implant surgical guides in tooth-supported PA and FA surgical guides. Each guide was developed in three thicknesses

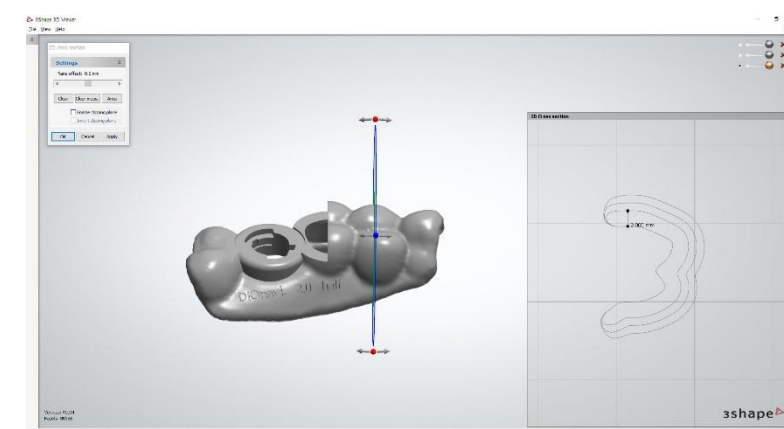
(2, 3, and 4 mm) and categorized into six groups according to arch type. Eight surgical guides were allocated to each group, generating a total of 48 guides used in the study. Storage durations were set at 0, 1, 3, 7, and 14 days. To maintain consistency across groups, an identical computer-aided design (CAD) was applied during guide fabrication.

2.2. CAD Design of Surgical Guides

The surgical guides were established using 3Shape Implant Studio (3Shape, Copenhagen, Denmark), according to data obtained from direct scanning of a model with a single missing tooth. Each guide was exported as an STL file for 3D printing. Two arch spans were developed: PA guides (Figure 2 B) covering a segment of the dentition, and FA guides (Figure 2 A) spanning the entire dental arch.



(A) Cross-sectional view illustrating the reference area for thickness measurement in the FA surgical guide design



(B) Cross-sectional view illustrating the reference area for thickness measurement in the PA surgical guide design

Fig. 2. Thickness measured from the outer contour of the guide body, excluding the sleeve

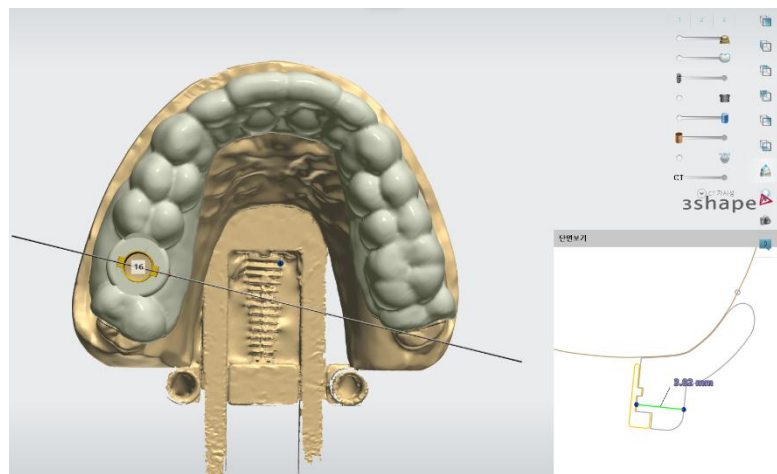


Fig. 3. Cross-sectional measurement of sleeve wall thickness (3.02 mm) in the surgical guide design

2.3. 3D Printing Protocol

The guide thickness was defined based on the outer surface of the main structure (Figure 2), excluding the sleeve. All thickness conditions (2, 3, and 4 mm) were developed along a common baseline. The sleeve thickness (Figure 3) was kept constant across all guides, with structural variations based on thickness applied only to the outer surface of the guide body. Fabrication of each guide was performed following standardized printing protocols.

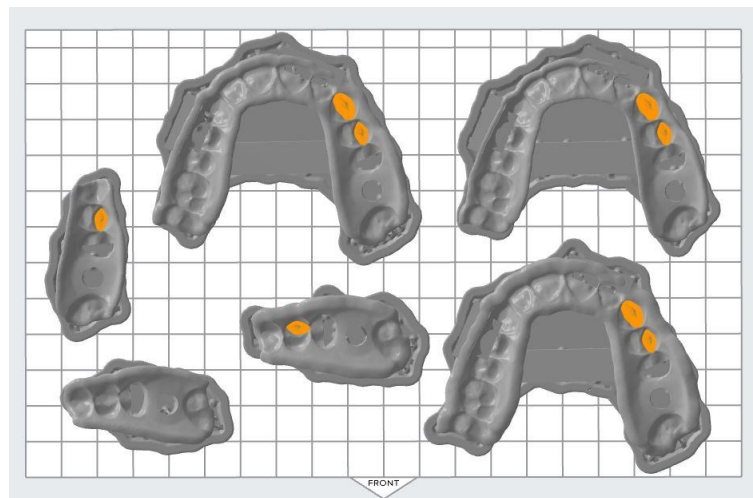


Fig. 4. Printing orientation of surgical guides at a 180° angle relative to the build platform

The surgical guides were printed using an SLA 3D printer (Form 4; Formlabs, Somerville, MA, USA) with a photopolymer resin (Gray Resin V5; Formlabs). Printing conditions were applied following the manufacturer's specifications. The printing orientation was set at a 180° angle relative to the build platform to optimize accuracy and reduce the risk of layer distortion (Figure 4). Eight guides were printed per group, with a randomized positioning employed in each printing cycle to reduce potential bias. Several previous studies have revealed that surgical guides established with a 50- μm layer thickness exhibit superior dimensional accuracy compared with those printed at 100 μm , thereby improving implant placement precision (34, 35). Based on these results, a 50- μm layer thickness was selected for the present study. Support structures were automatically generated utilizing Formlabs PreForm software, with a 0.35-mm minimum support density and a 0.6-mm post-printing touchpoint size.

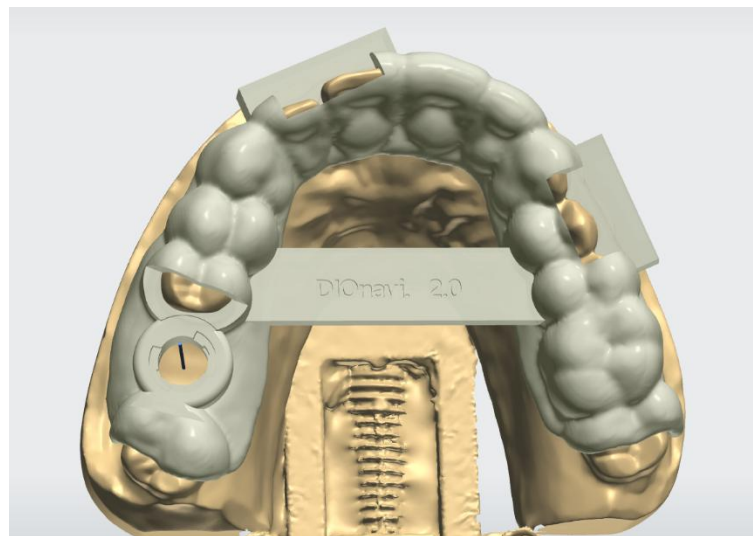


Fig. 5. Partial-arch surgical template

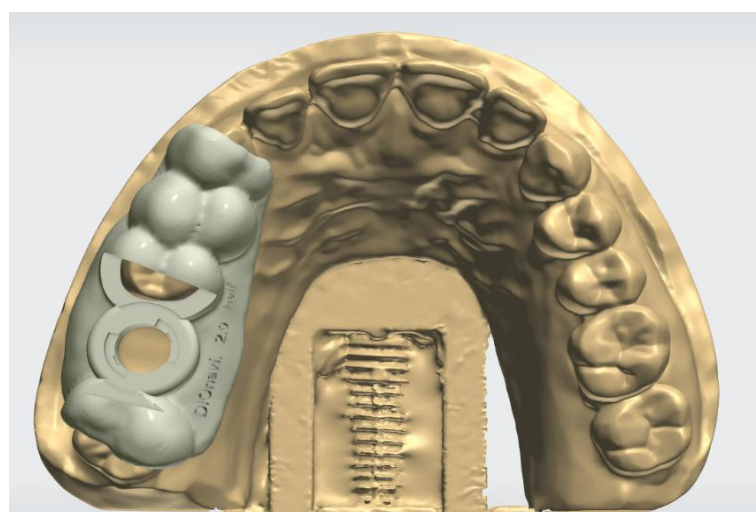


Fig. 6. Full-arch surgical template

2.4. Storage Conditions and Measurement Schedule

The implant placement location was standardized at the right maxillary first molar for both PA and FA guides. A supplementary support structure was incorporated to improve guide stability and minimize deformation. The FA guide was designed to cover the entire dentition, including the first and second molars bilaterally. A connecting bar was then added between the left and right molars to improve structural rigidity and resistance to deformation. In contrast, the PA guide was locally designed to accommodate the adjacent teeth around the missing right maxillary first molar. This design was optimized to enable comparative analysis of structural stability and deformability in the two configurations.

After the printing process, all surgical guides were ultrasonically cleaned in 95% isopropyl alcohol (IPA) for 5 min and post-cured for 15 min utilizing a UV curing unit (Form Cure; Formlabs) at 60°C. Post-curing was performed to ensure sufficient mechanical strength and dimensional stability. After curing, precision cutters were used to carefully remove all support structures to avoid inducing surface damage, and the guides were labeled and prepared for subsequent experimental procedures.

The surgical guides were stored in a sealed drawer under controlled environmental conditions ($22 \pm 2^\circ\text{C}$, $50\% \pm 5\%$ relative humidity) to minimize the effects of external variables on dimensional stability. These conditions were selected following the resin manufacturer's recommendations, as temperature and humidity fluctuations have caused polymer relaxation and post-curing shrinkage in 3D-printed photopolymer materials. The guides were retrieved from storage only at predetermined measurement intervals (0, 1, 3, 7, and 14 days) to ensure consistent handling and minimize unintended light and moisture exposure.

2.5. Dimensional Analysis and Scanning Protocol

Medit ColLab software and a desktop scanner (Medit T500; Medit Corp., Seoul, S. Korea) were used to scan surgical guides for each time point. Each group was scanned once per interval, and the obtained datasets were averaged to quantify deformation. PA and FA guides were simultaneously scanned to reduce potential measurement bias related to handling or storage. Metrology software (Geomagic Control X; 3D Systems Inc., Rock Hill, SC, USA) was used to superimpose the scan data on the original CAD model, and root mean square error (RMSE) values were calculated. A color map analysis was subsequently conducted to assess spatial deformation patterns concerning guide thickness, arch span, and storage duration.

2.6. Seating Accuracy Analysis

Each guide was mounted on the corresponding model to assess seating accuracy, and spherical reference markers were embedded into the design to create consistent coordinate references.



Quantitative analysis of seating deviation was conducted by comparing the actual positions of the markers to the design reference points.

2.7. Statistical Analysis

SAS software (SAS Institute Inc., Cary, NC, USA) was used for statistical analyses. A three-way analysis of variance (ANOVA) was conducted to assess the main effects and interactions among thickness, arch type, and storage duration. Tukey's post hoc test was employed to determine significant differences among groups, with statistical significance set at $\alpha = 0.05$. The mean and standard deviation of RMSE values were calculated for each group to evaluate the statistical relevance of observed deformation patterns.

3. RESULTS

3.1. Dimensional Stability (RMSE Results)

The RMSE, indicating the trueness of 3D-printed surgical guides, was analyzed concerning arch span (Partial vs. Full), guide thickness (2, 3, and 4 mm), and recording date (day 0 to day 14). Lower RMSE values reflect better similarity to the virtual design, thereby indicating higher dimensional accuracy.

Three-way ANOVA revealed significant primary effects of recording date ($p < 0.001, F = 15.708$) and thickness ($p < 0.001, F = 89.531$), whereas the main effect of arch span was not statistically significant ($p = 0.290, F = 1.127$). Notably, significant interactions were found between date and thickness ($p < 0.001, F = 23.742$), arch and thickness ($p < 0.001, F = 101.874$), date and arch ($p < 0.001, F = 33.275$) and among the three-way interaction of date, arch, and thickness ($p < 0.001, F = 25.932$). This indicates that both the individual factors and their combined interactions contributed to variations in trueness.

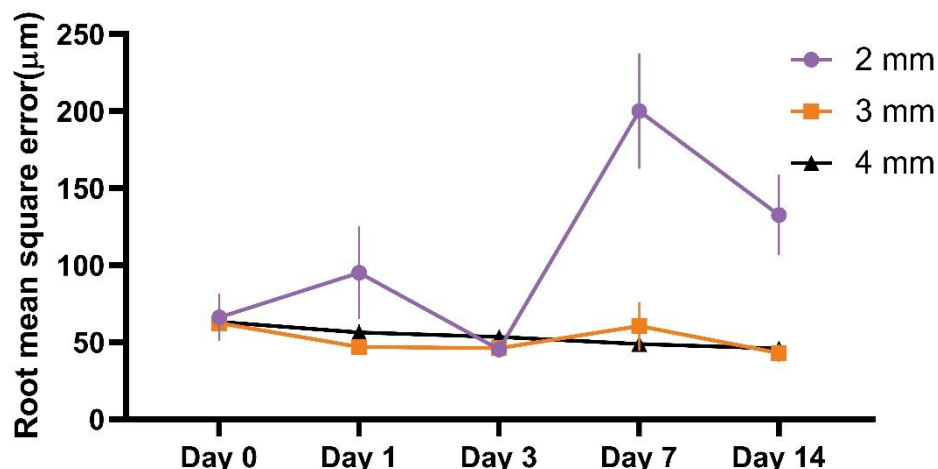


Figure 7. Time-dependent changes in RMSE across different guide thicknesses under the partial-arch design

Table 1. Root mean square error values of 3D-printed surgical guides with partial arch over 14 days

| | Day 0 | Day 1 | Day 3 | Day 7 | Day 14 |
|------|--------------------------------|-------------------------------|------------------------------|--------------------------------|--------------------------------|
| 2 mm | $66.24 \pm 15.24^{\text{Aab}}$ | $95.16 \pm 30.16^{\text{Bb}}$ | $45.24 \pm 5.42^{\text{Aa}}$ | $200.14 \pm 37.52^{\text{Bd}}$ | $132.56 \pm 26.28^{\text{Bc}}$ |
| 3 mm | $62.40 \pm 10.42^{\text{Aa}}$ | $46.88 \pm 3.49^{\text{Aa}}$ | $46.24 \pm 3.66^{\text{Aa}}$ | $60.48 \pm 15.72^{\text{Aa}}$ | $42.94 \pm 5.78^{\text{Aa}}$ |
| 4 mm | $63.16 \pm 4.64^{\text{Aa}}$ | $56.32 \pm 5.24^{\text{Aa}}$ | $53.46 \pm 4.04^{\text{Aa}}$ | $48.82 \pm 4.36^{\text{Aa}}$ | $45.90 \pm 3.73^{\text{Aa}}$ |

Uppercase letters indicate statistically significant differences among thickness groups ($p < 0.05$), whereas lowercase letters denote significant differences across recording dates ($p < 0.05$).

Accordingly, post-hoc analyses were conducted for PA and FA designs. RMSE values were more variable over time in the PA group, particularly in the 2-mm group (Figure 7). The RMSE of the 2-mm guides increased from $66.24 \pm 15.24 \mu\text{m}$ on day 0 to $200.14 \pm 37.52 \mu\text{m}$ on day 7, followed by a decrease to $132.56 \pm 26.28 \mu\text{m}$ on day 14 (Table 1). These values were significantly higher than those of the 3-mm (day 1: $46.88 \pm 3.49 \mu\text{m}$; day 7: $60.48 \pm 15.72 \mu\text{m}$; day 14: $42.94 \pm 5.78 \mu\text{m}$) and 4-mm (day 1: $56.32 \pm 5.24 \mu\text{m}$; day 7: $48.82 \pm 4.36 \mu\text{m}$; day 14: $45.90 \pm 3.73 \mu\text{m}$) groups at the same time point ($p < 0.05$). Further, significant differences were observed among recording dates within the 2-mm group ($p < 0.05$), with the most pronounced increase occurring between day 3 and day 7. In contrast, RMSE values in the 3-mm and 4-mm groups remained relatively stable throughout the observation period (range: $42.94\text{--}63.16 \mu\text{m}$), with no significant time-dependent deviation.

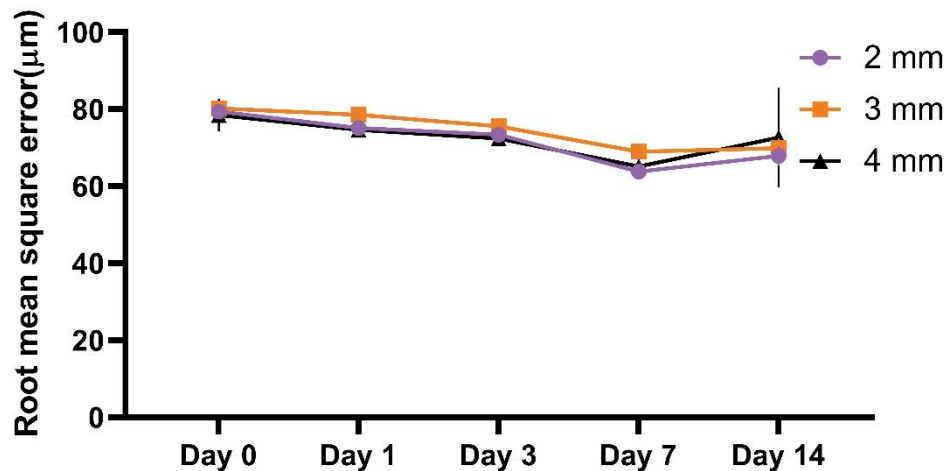


Figure 8. Time-dependent changes in RMSE across different guide thicknesses under the full-arch design

Table 2. Root mean square error values of 3D-printed surgical guides with full-arch over 14 days

| | Day 0 | Day 1 | Day 3 | Day 7 | Day 14 |
|------|------------------------------|-------------------------------|-------------------------------|------------------------------|--------------------------------|
| 2 mm | $79.34 \pm 0.63^{\text{Ab}}$ | $75.14 \pm 1.53^{\text{Ab}}$ | $73.38 \pm 0.78^{\text{Aa}}$ | $63.76 \pm 0.30^{\text{Aa}}$ | $67.90 \pm 2.43^{\text{Aa}}$ |
| 3 mm | $80.24 \pm 1.12^{\text{Ab}}$ | $78.56 \pm 0.38^{\text{Ab}}$ | $75.50 \pm 2.05^{\text{Aab}}$ | $68.96 \pm 0.59^{\text{Aa}}$ | $69.90 \pm 2.51^{\text{Aa}}$ |
| 4 mm | $78.48 \pm 4.20^{\text{Ac}}$ | $74.62 \pm 1.37^{\text{Abc}}$ | $72.40 \pm 0.49^{\text{Abc}}$ | $65.16 \pm 0.47^{\text{Aa}}$ | $72.60 \pm 12.93^{\text{Abc}}$ |

Uppercase letters indicate statistically significant differences among thickness groups ($p < 0.05$), whereas lowercase letters denote significant differences across recording dates ($p < 0.05$).

Overall RMSE values were lower and demonstrated minimal temporal change in the FA group (Figure 8). RMSE values decreased from 79.34 ± 0.63 μm on day 0 to 63.76 ± 0.30 μm on day 7 and slightly increased to 67.90 ± 2.43 μm on day 14 in the 2-mm group (Table 2). Similar mild fluctuations were observed in the 3-mm (from 80.24 ± 1.12 μm to 68.96 ± 0.59 μm) and 4-mm (from 78.48 ± 4.20 μm to 65.16 ± 0.47 μm) groups. No statistically significant differences were observed between thickness groups or recording dates ($p > 0.05$)

3.2. Color Map Analysis of Deformation Patterns

Figure 9 illustrates the dimensional deviation using the “3D Compare function” in Geomagic Control X. In PA guides, red regions that indicate positive deviations were consistently more prominent than blue regions across 3-mm and 4-mm thicknesses, with deviation localized mainly at the intaglio and marginal surfaces. The blue regions in 2-mm thickness gradually exceeded the red regions after day 7. In contrast, FA guides demonstrated extensive blue regions, indicating negative deviation, particularly along the intaglio and palatal areas.

To quantitatively assess dimensional deviation, the colormap images corresponding to each time point (days 0, 1, 3, 7, and 14) were separated into individual frames for analysis. Each image was processed in RStudio (version 2024.12.1+563) and converted to the HSV (Hue, Saturation, Value) color space to facilitate pixel-level color classification.

The surgical guide was isolated from the background by first applying a grayscale-based mask. Red and blue regions within the guide were determined based on empirically defined hue thresholds derived from the reference colormap: red tones correspond to positive deviations ($\Delta > +0.05$ mm; hue $\approx 0.00\text{--}0.15$), and blue tones denote negative deviations ($\Delta < -0.05$ mm; hue $\approx 0.47\text{--}0.89$). To avoid the inclusion of desaturated or dark pixels, only those with saturation and brightness above defined thresholds ($S > 0.2$, $V > 0.2$) were considered.

The number of pixels falling within each deviation range was counted and presented as a total guide area proportion. Figure 10 illustrates the segmented red and blue deviation areas for each observation day, and temporal changes in these regions were used to assess the progression of dimensional stability.

Quantitative assessment of red and blue area ratios (Figure 11) confirmed these observations. Red areas were consistently larger than blue areas in 3-mm and 4-mm PA groups, indicating a predominance of positive deviation. Red area ratios in 3-mm and 4-mm PA remained relatively stable over time (7%–8%), whereas blue area ratios fluctuated around or below 3%. Conversely, blue regions were more extensive than red in all designs in FA groups, especially in 2-mm and 4-mm FA, where blue area ratios exceeded 30% at multiple timepoints. The 3-mm FA group demonstrated a moderate and gradual decrease in blue-region deviations, whereas the red region remained relatively constant (18%–20%).

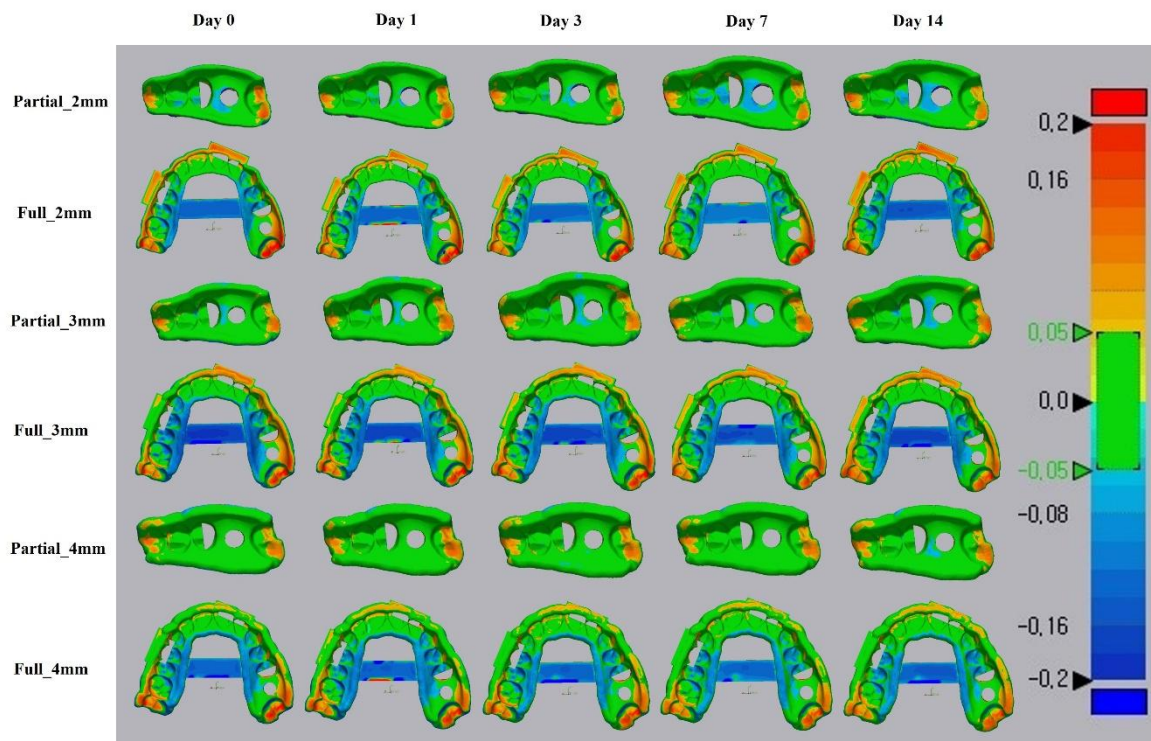


Figure 9. Colormap of dimensional deviation in 3D-printed surgical guides

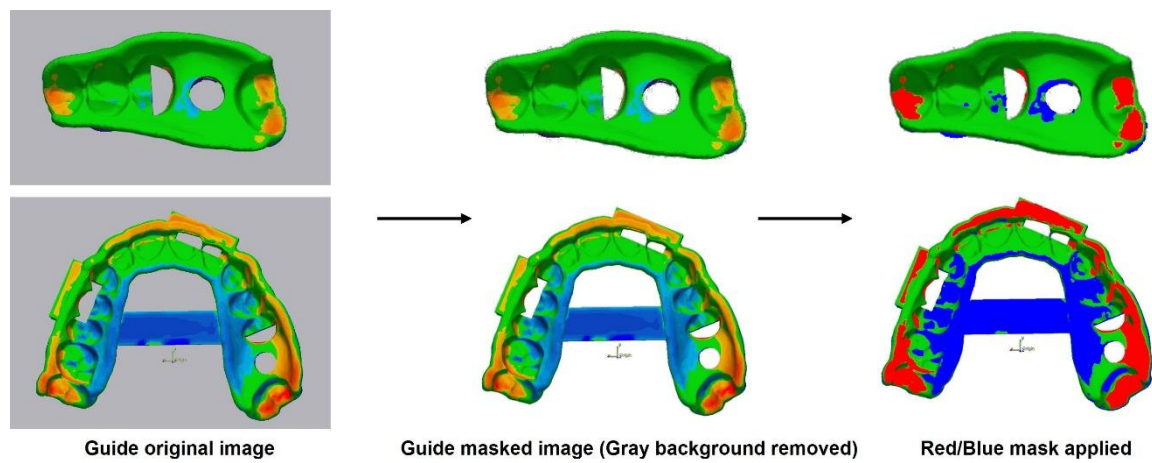


Figure 10. Workflow of colormap segmentation and area extraction

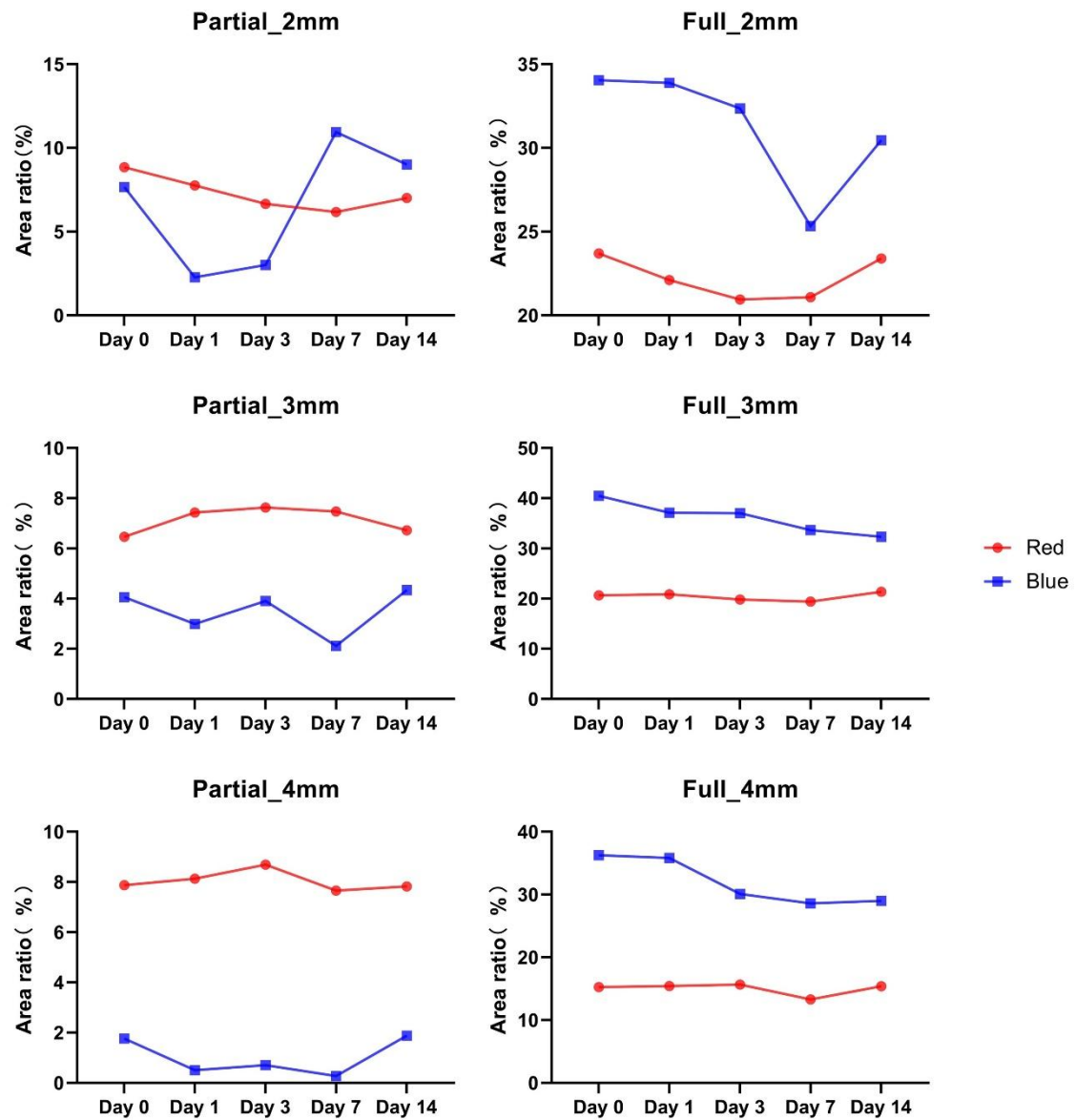


Figure 11. Time-dependent changes in red and blue area ratios extracted from colormaps for different surgical guide designs and thicknesses. Blue and red regions represent deviations below -0.05 mm and above $+0.05$ mm, respectively.

3.3. Seating Accuracy

Three-way ANOVA results for seating accuracy revealed significant main effects of arch span ($p < 0.001, F = 49.178$), recording date ($p < 0.001, F = 6.385$), and guide thickness ($p = 0.036, F = 3.415$). Further, significant interactions were found between arch and recording date ($p < 0.001, F = 5.870$), recording date and thickness ($p < 0.001, F = 5.373$), arch span and thickness ($p = 0.008, F = 4.988$), and among arch span, thickness, and recording date ($p < 0.001, F = 5.528$). This indicates that both the individual effects and their combined interactions contributed to variations in seating accuracy.

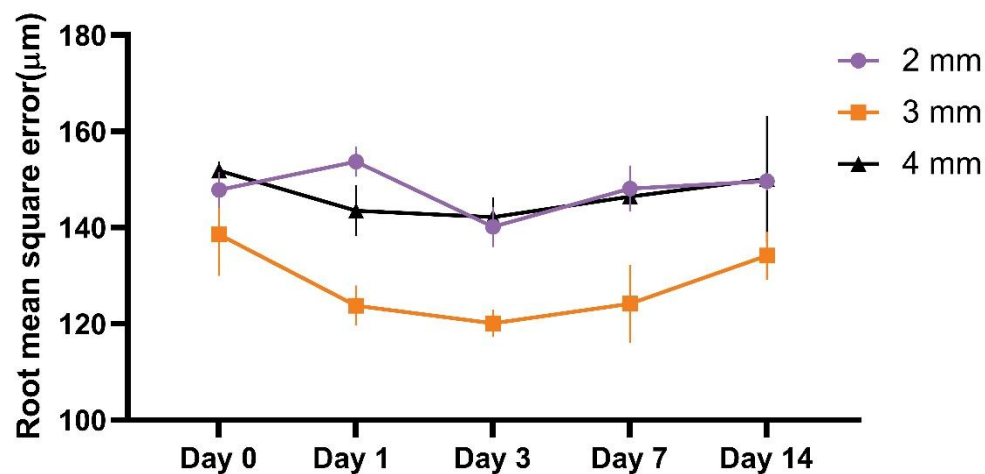


Figure 12. Time-dependent changes in seating accuracy across different guide thicknesses under the partial-arch design

Table 3. Seating accuracy of 3D-printed surgical guides with partial-arch design over 14 days

| | Day 0 | Day 1 | Day 3 | Day 7 | Day 14 |
|------|-------------------------------|-------------------------------|-------------------------------|-------------------------------|--------------------------------|
| 2 mm | $147.82 \pm 3.71^{\text{Bb}}$ | $153.72 \pm 3.15^{\text{Cb}}$ | $140.14 \pm 4.14^{\text{Ba}}$ | $148.12 \pm 4.80^{\text{Bb}}$ | $149.62 \pm 1.83^{\text{Bb}}$ |
| 3 mm | $138.54 \pm 8.55^{\text{Ac}}$ | $123.80 \pm 4.17^{\text{Ab}}$ | $120.12 \pm 2.83^{\text{Aa}}$ | $124.16 \pm 8.14^{\text{Ab}}$ | $134.16 \pm 4.97^{\text{Abc}}$ |
| 4 mm | $151.82 \pm 1.90^{\text{Ba}}$ | $143.52 \pm 5.31^{\text{Ba}}$ | $142.14 \pm 4.13^{\text{Ba}}$ | $146.44 \pm 2.70^{\text{Ba}}$ | $150.12 \pm 13.12^{\text{Ba}}$ |

Uppercase letters indicate statistically significant differences among thickness groups ($p < 0.05$), whereas lowercase letters indicate significant differences across recording dates ($p < 0.05$).

RMSE values in the PA group remained relatively consistent across time, ranging from $140.14 \pm 4.14 \mu\text{m}$ to $153.72 \pm 3.15 \mu\text{m}$ in the 2 mm and from $120.12 \pm 2.83 \mu\text{m}$ to $138.54 \pm 8.55 \mu\text{m}$ in the 3 mm groups (Table 3). The 3 mm guides consistently exhibited the lowest RMSE across all time points, with statistically significant differences compared with 2-mm and 4-mm guides on multiple dates ($p < 0.05$), indicating better seating accuracy (Figure 12). Post-hoc comparisons for thickness over time indicated significant initial decreases in RMSE, followed by slight increases at later recording dates ($p < 0.05$).

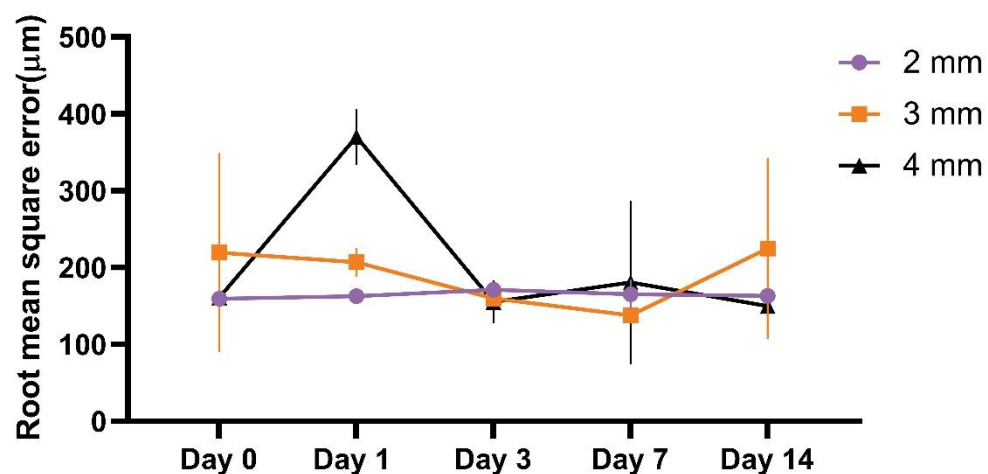


Figure 13. Time-dependent changes in seating accuracy across different guide thicknesses under the full-arch design

Table 4. Seating accuracy of 3D-printed surgical guides with full-arch design over 14 days

| | Day 0 | Day 1 | Day 3 | Day 7 | Day 14 |
|------|---------------------------------|--------------------------------|--------------------------------|---------------------------------|---------------------------------|
| 2 mm | $159.48 \pm 3.75^{\text{Aa}}$ | $162.58 \pm 5.09^{\text{Aa}}$ | $170.88 \pm 9.93^{\text{Aa}}$ | $165.36 \pm 18.89^{\text{Aa}}$ | $163.28 \pm 3.48^{\text{Aa}}$ |
| 3 mm | $219.56 \pm 129.23^{\text{Aa}}$ | $206.70 \pm 19.03^{\text{Aa}}$ | $159.92 \pm 5.56^{\text{Aa}}$ | $137.70 \pm 4.70^{\text{Aa}}$ | $224.80 \pm 117.32^{\text{Aa}}$ |
| 4 mm | $160.84 \pm 22.78^{\text{Aa}}$ | $370.12 \pm 36.04^{\text{Bb}}$ | $155.32 \pm 27.98^{\text{Aa}}$ | $180.66 \pm 106.35^{\text{Aa}}$ | $149.80 \pm 15.28^{\text{Aa}}$ |

Uppercase letters indicate statistically significant differences among thickness groups ($p < 0.05$), whereas lowercase letters denote significant differences across recording dates ($p < 0.05$).

Greater variability was observed in the FA group. Notably, the 4-mm group demonstrated a spike

in RMSE at day 1 ($370.12 \pm 36.04 \mu\text{m}$), which was significantly higher than all other groups ($p < 0.05$), followed by a return to baseline until day 14 ($149.80 \pm 15.28 \mu\text{m}$) (Figure 13). In contrast, the 2-mm and 3-mm groups maintained relatively stable RMSE values throughout the observation period (2 mm: $159.48 \pm 3.75 \mu\text{m}$ to $170.88 \pm 9.93 \mu\text{m}$; 3 mm: $159.92 \pm 5.56 \mu\text{m}$ to $224.80 \pm 117.32 \mu\text{m}$), without significant time-dependent variations ($p > 0.05$) (Table 4).

Figure 14 illustrates the colormap of seating accuracy. Deviations in the PA groups were primarily localized to the posterior segments, particularly at the molar regions, whereas the anterior regions maintained relatively high congruency throughout all observation periods. Notably, deviations in the FA groups demonstrated a broader distribution, frequently extending bilaterally across the entire arch span, with negative deviations observed along the guide edge areas and positive deviations in the occlusal regions.

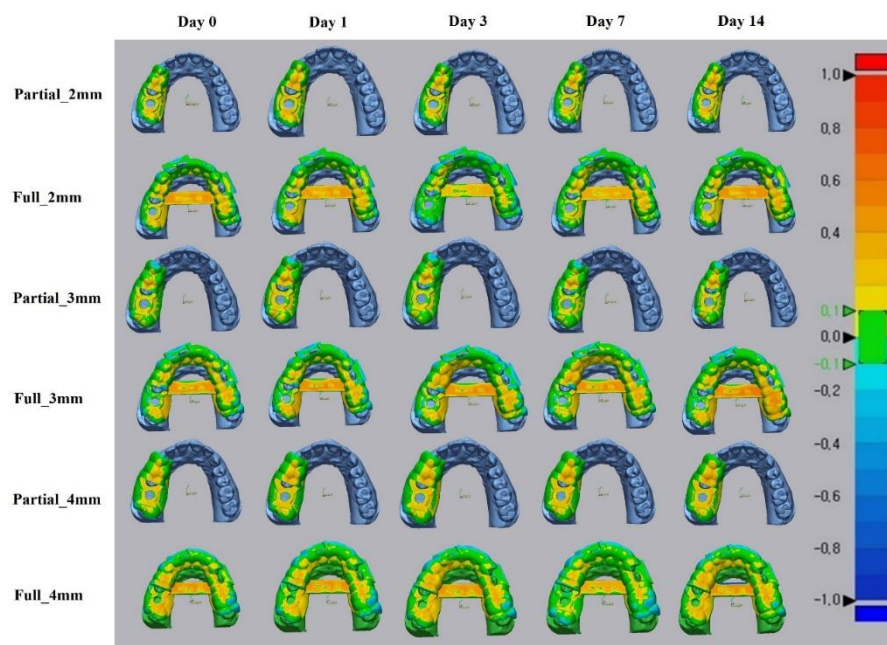


Figure 14. Colormap of dimensional deviation in 3D-printed surgical guides when seated on a dental model cast

4. DISCUSSION

The null hypothesis stating that surgical guide thickness, arch span length, and storage duration would exhibit no significant effects on dimensional deformation and seating accuracy was only partially rejected. Both guide thickness and arch configuration demonstrated statistically significant effects on deformation and seating accuracy, particularly in thinner PA guides; however, storage duration did not substantially increase deformation beyond the initial post-curing stabilization period.

Previous studies have indicated the importance of thorough preoperative planning in achieving successful implant treatment (36). Such planning helps prevent unanticipated complications and improve the predictability of treatment outcomes. However, surgical guide deformation may hinder the intended treatment even with meticulous planning. Several studies have revealed that the manufacturing method, material, printing orientation (37), and storage conditions affect the accuracy of surgical guides (30, 38, 39). Deformation is indicated to increase over time under certain conditions (40). In the present study, most guides demonstrated stable dimensional characteristics after initial post-curing; however, a sharp increase in deformation was observed in the 2-mm PA guide, particularly at day 7. This implies that structural stability may degrade over time according to design variables, and that time-related deformation cannot be generalized across all conditions. Therefore, clinical application requires careful consideration of both guide form and thickness in terms of time-dependent effects.

This study assesses the effect of storage duration on the dimensional stability and deformability of implant surgical guides to evaluate the potential effect of long-term storage on surgical accuracy. The results revealed that increasing guide thickness was related to decreased deformation and improved structural stability, particularly in PA guides with narrower support spans. These results experimentally support previous finite element analysis studies indicating that increased thickness improves internal stress distribution and deformation resistance (41, 42). However, excessively thick guides may compromise patient comfort and procedural efficiency due to increased material usage and weight. Therefore, structural stability and clinical practicality must be consistently balanced. From this perspective, designing surgical guides with a 3-mm minimum thickness is considered advisable.

Previous studies have reported that deformation progressively increases during long-term storage, especially at the mucosal contact surface (26); however, the present study revealed no consistent trend across all conditions. Significant deformation after day 7 was observed only in the 2-mm PA group, indicating that time-dependent deformation patterns vary with guide geometry and thickness. These results indicate the need for condition-specific assessment rather than general assumptions. This study provides practical data for optimizing the clinical timing of surgical guide use, considering both thickness and storage duration, despite the limited number of studies that have quantitatively assessed time-dependent deformation based on thickness.

This study comprehensively analyzed the effects of guide thickness, arch span, and storage duration on both deformation and seating accuracy. The initial hypothesis stating that these factors would not significantly affect dimensional accuracy was only partially supported. Thickness and storage duration significantly influenced both deformation and seating precision.

RMSE analysis revealed that the 2-mm PA guide demonstrated the highest deformation, with a peak of $200.14 \pm 37.52 \mu\text{m}$ on day 7. In contrast, the 3-mm and 4-mm groups maintained stable deformation levels below $60 \mu\text{m}$. FA guides displayed relatively small and consistent deformation across all thicknesses, with no significant time-dependent variation. These results indicate that the limited support area of PA guides and the reduced thickness in the 2-mm groups make them more vulnerable to external stress. Conversely, the FA design, supported bilaterally with a cross bar, may contribute to improved dimensional stability.

These trends were observed in the color map-based quantitative analysis. The PA groups demonstrated a higher proportion of red areas, indicating expansion, whereas the FA groups exhibited broader blue regions, reflecting shrinkage. In particular, $>30\%$ of the surface area in the 2-mm and 4-mm FA groups demonstrated shrinkage regions, implying the possibility of internal stress reduction during storage. Meanwhile, the 3-mm and 4-mm PA groups consistently maintained expansion-dominated regions, indicating relatively stable internal structures.

Seating accuracy analysis revealed both thickness and arch span as key variables. The 3-mm PA guide demonstrated the lowest deviation across all time points, indicating excellent seating performance and consistent with its dimensional stability. In contrast, the 4-mm FA guide showed a temporary increase in error ($370.12 \pm 36.04 \mu\text{m}$) on day 1, which may be attributed to transient deformation due to post-curing contraction or localized stress concentration.

The three-way ANOVA revealed that thickness, arch span, and storage duration individually and interactively affected both RMSE and seating accuracy. This indicates that guide design should not depend on single-factor assumptions but rather incorporate multifactorial considerations. Before clinical use, an appropriate stabilization period following printing and post-curing should be enabled. In particular, deformation-sensitive designs, such as FA guides, should be fabricated with sufficient thickness to ensure both structural stability and clinical precision.

This study confirmed a trend of reduced deformation with increased guide thickness, which supports the hypothesis stating that thicker structures promote uniform internal stress distribution and improve environmental factor resistance (29, 32). Notably, the 4-mm PA guide consistently demonstrated lower RMSE values than the 2-mm and 3-mm groups, thereby maintaining dimensional stability throughout the storage period. These results underscore the role of guide thickness as a crucial design factor for minimizing deformation.

Conversely, the hypothesis stating that prolonged storage exhibited negligible effects on guide deformation was only partially validated. Most deformation occurred during the immediate post-

curing phase and stabilized thereafter, with minimal additional changes in the 14-day storage period. This is consistent with previous studies indicating that deformation primarily occurs during the initial stabilization phase, with negligible changes beyond 20 days (26). However, the sharp deformation increase observed on day 7 in the 2-mm PA group indicates that guide geometry and thickness affected time-related deformation. Moreover, the deformation levels reported in previous studies (26) and the RMSE range observed in this study (45–70 μm) fall within clinically acceptable limits, which supports the applicability of these guides in practice. The results highlight the importance of standardizing post-curing protocols and storage environments to minimize early deformation, which is considered a foundation for establishing clinical guidelines for surgical guide fabrication.

Discrepancies between this study and those of previous research may be attributed to experimental variables such as the type of photopolymer resin, printing parameters, post-processing methods, and measurement techniques (31, 41–45). These differences may account for variations in the result. Therefore, further standardized studies using various materials and fabrication protocols are warranted to improve clinical reliability. Most deformation occurred within the first few days after printing and stabilized during subsequent storage in clinical practice. This is congruent with previous results indicating that deformation in photocurable resins primarily occurs during the initial post-curing stage (46) and stabilizes thereafter (47–49). Further, photopolymer materials may be susceptible to environmental changes, such as UV light and humidity (50–53), thereby supporting the need for a stabilization period and controlled storage conditions to preserve guide accuracy.

Moreover, this study revealed that deformation patterns differed based on the arch span, with FA guides demonstrating greater deformation than PA guides. This indicates that a greater arch span results in more complex stress distribution, thereby reducing structural stability. Therefore, increasing thickness or incorporating additional reinforcement may be required to improve the dimensional stability of FA designs.

Previous studies have revealed that the structural configuration of surgical guides, particularly the distinction between fully and partially guided designs, significantly affects implant placement accuracy (54). The overall deformation levels in this study were within clinically acceptable limits, although minor deformation in thinner or longer-span guides may affect implant accuracy. Therefore, a minimum guide thickness of at least 4 mm is advisable to be maintained, and sufficient reinforcement should be ensured, especially in FA applications.

The observed deformation changes during the storage period may be statistically significant, but they may not be clinically relevant. Most deformation occurred early and then stabilized. Therefore, post-curing process optimization and appropriate storage condition maintenance are crucial to minimizing initial deformation and improving clinical utility.

This study has several limitations. First, the application of a single material and a single printing method (SLA) may limit generalizability. SLA is widely used due to its high precision; however,

previous studies have demonstrated that post-curing and storage may still induce deformation in photopolymerized resins (26, 31, 50). Such deformation may cause discrepancies between planned and actual implant positions. Additional research using different materials and printing techniques is warranted. Second, experiments were conducted in a controlled laboratory setting, which may not fully replicate clinical environments. Therefore, further research needs to assess deformation in real-world clinical contexts. Third, the storage duration in this study was limited to 14 days. Longer-term studies are warranted to assess extended stability. Future research needs to include prolonged observation periods and diverse printing parameters to improve generalizability and confirm clinical reliability.

However, this study holds academic significance in that it systematically assessed the effects of guide thickness and storage duration on surgical guide deformation. Unlike previous studies that focused on manufacturing methods or material properties, this study quantitatively evaluated deformation patterns under consistent conditions and determined the early post-curing deformation and stabilization trend during storage. A unique contribution of this study is its comparison of PA and FA configurations to assess the effects of structural variation on dimensional stability.

In conclusion, this study experimentally revealed that increasing guide thickness improves dimensional stability and reduces deformation. Deformation in most conditions occurred during the initial post-curing phase and remained stable throughout the 14-day storage period. Clinically, a minimum thickness of ≥ 3 mm is recommended to be ensured, and an appropriate stabilization period needs to be enabled following printing to minimize deformation and improve implant placement accuracy.



5. CONCLUSION

This study revealed no significant time-dependent dimensional changes in most thickness and arch span groups, especially in guides with a ≥ 3 -mm thickness, which consistently demonstrated stable deformation patterns throughout the storage period. However, partial arch surgical guides with a 2-mm thickness demonstrated a notable increase in deformation around day 7, indicating that thinner structures may be more susceptible to external stress.

Most dimensional changes occurred between days 0 and 1, emphasizing the crucial importance of the immediate post-curing phase in achieving dimensional stability. These results indicate that securing sufficient post-curing and stabilization time after fabrication is essential to minimize deformation and improve clinical accuracy. A 3-mm minimum guide thickness is recommended, with 4 mm being preferable in partial arch designs to ensure greater structural reliability.

REFERENCES

1. Dawood, A., Marti, B. M., Sauret-Jackson, V., & Darwood, A. (2015). 3D printing in dentistry. *British Dental Journal*, 219(11), 521–529. <https://doi.org/10.1038/sj.bdj.2015.914>
2. Shaker, I., & Elkady, D. (2024). Accuracy of two 3D printing technologies in manufacturing of dental implant surgical guides (An in vitro study). *Egyptian Journal of Oral and Maxillofacial Surgery*, 15(1), 6–10. <https://doi.org/10.21608/omx.2024.251878.1212a>
3. Pradíes, G., Morón-Conejo, B., Martínez-Rus, F., Salido, M. P., & Berrendero, S. (2024). Current applications of 3D printing in dental implantology: A scoping review mapping the evidence. *Clinical Oral Implants Research*, 35(8), 1011–1032. <https://doi.org/10.1111/clr.14198>
4. Rouzé l'Alzit, F., Cade, R., Naveau, A., Babilotte, J., Meglioli, M., & Catros, S. (2022). Accuracy of commercial 3D printers for the fabrication of surgical guides in dental implantology. *Journal of Dentistry*, 117, 103909. <https://doi.org/10.1016/j.jdent.2021.103909>
5. Dahmani, I., & Ghazi, M. E. (2024). Digital workflow for full arch rehab and surgical guide for implant placement. *Journal of Dentistry*, 147, 105202. <https://doi.org/10.1016/j.jdent.2024.105202>
6. Sarment, D. P., Sukovic, P., & Clinthorne, N. (2003). Accuracy of implant placement with a stereolithographic surgical guide. *International Journal of Oral & Maxillofacial Implants*, 18(4), 571.
7. Giacomo, G. A. P. D., Cury, P. R., de Araujo, N. S., Sendyk, W. R., & Sendyk, C. L. (2005). Clinical application of stereolithographic surgical guides for implant placement: Preliminary results. *Journal of Periodontology*, 76(4), 503–507. <https://doi.org/10.1902/jop.2005.76.4.503>
8. Zoabi, A., Redenski, I., Oren, D., Kasem, A., Zigron, A., Daoud, S., Moskovich, L., Kablan, F., & Srouji, S. (2022). 3D printing and virtual surgical planning in oral and maxillofacial surgery. *Journal of Clinical Medicine*, 11(9), 2385. <https://doi.org/10.3390/jcm11092385>
9. Turkyilmaz, I., & Wilkins, G. N. (2021). 3D printing in dentistry – Exploring the new horizons. *Journal of Dental Sciences*, 16(3), 1037–1038. <https://doi.org/10.1016/j.jds.2021.04.004>
10. Abad-Coronel, C., Vandeweghe, S., Vela Cervantes, M. D., Tobar Lara, M. J., Mena Córdova, N., & Aliaga, P. (2024). Accuracy of implant placement using digital prosthetically-derived surgical guides: A systematic review. *Applied Sciences*, 14(16), 7422. <https://doi.org/10.3390/app14167422>

11. Deepa, K. S. (2022). Surgical guides in implantology: A realistic approach towards precision. *IP International Journal of Maxillofacial Imaging*, 8(3), 101–105. <https://doi.org/10.18231/j.ijmi.2022.024>
12. Li, H., Eo, M. Y., Mustakim, K. R., & Kim, S. M. (2024). A 10-year follow-up study on clinical outcomes of dental implant rehabilitation using surgical guide. *Journal of the Korean Association of Oral and Maxillofacial Surgeons*, 50(2), 70–79. <https://doi.org/10.5125/jkaoms.2024.50.2.70>
13. Walker-Finch, K., & Ucer, C. (2020). Five-year survival rates for implants placed using digitally-designed static surgical guides: A systematic review. *British Journal of Oral and Maxillofacial Surgery*, 58(3), 268–276. <https://doi.org/10.1016/j.bjoms.2019.12.007>
14. Putra, R. H., Yoda, N., Astuti, E. R., & Sasaki, K. (2022). The accuracy of implant placement with computer-guided surgery in partially edentulous patients and possible influencing factors: A systematic review and meta-analysis. *Journal of Prosthodontic Research*, 66(1), 29–39. https://doi.org/10.2186/jpr.jpr_d_20_00184
15. Kessler, A., Hickel, R., & Reymus, M. (2020). 3D printing in dentistry—State of the art. *Operative Dentistry*, 45(1), 30–40. <https://doi.org/10.2341/18-229-1>
16. Jeong, M., Radomski, K., Lopez, D., Liu, J. T., Lee, J. D., & Lee, S. J. (2023). Materials and applications of 3D printing technology in dentistry: An overview. *Dentistry Journal*, 12(1), 1. <https://doi.org/10.3390/dj12010001>
17. Tian, Y., Chen, C., Xu, X., Wang, J., Hou, X., Li, K., Lu, X., Shi, H., Lee, E.-S., & Jiang, H. B. (2021). A review of 3D printing in dentistry: technologies, affecting factors, and applications. *Scanning*, 2021(1), 1–19. <https://doi.org/10.1155/2021/9950131>
18. Tichá, D., Tomášik, J., Oravcová, L., & Thurzo, A. (2024). Three-dimensionally-printed polymer and composite materials for dental applications with focus on orthodontics. *Polymers*, 16(22), 3151. <https://doi.org/10.3390/polym16223151>
19. Lüchtenborg, J., Burkhardt, F., Nold, J., Rothlauf, S., Wesemann, C., Pieralli, S., Wemken, G., Witkowski, S., & Spies, B. C. (2021). Implementation of fused filament fabrication in dentistry. *Applied Sciences*, 11(14), 6444. <https://doi.org/10.3390/app11146444>
20. Grzebieluch, W., Grajzer, M., & Mikulewicz, M. (2023). Dimensional accuracy in dental models: An examination of fused deposition modeling versus digital light processing techniques for

clear aligner manufacturing. *Medical Science Monitor*, 29, e940922-1.
<https://doi.org/10.12659/msm.940922>

21. Németh, A., Vitai, V., Czumbel, M. L., Szabó, B., Varga, G., Kerémi, B., Hegyi, P., Hermann, P., & Borbély, J. (2023). Clear guidance to select the most accurate technologies for 3D printing dental models – A network meta-analysis☆. *Journal of Dentistry*, 134, 104532. <https://doi.org/10.1016/j.jdent.2023.104532>

22. Kim, H.-J., Lim, S.-W., Lee, M.-K., Ju, S. W., Park, S.-H., Ahn, J.-S., & Hwang, K.-G. (2021). Which three-dimensional printing technology can replace conventional manual method of manufacturing oral appliance? A preliminary comparative study of physical and mechanical properties. *Applied Sciences*, 12(1), 130. <https://doi.org/10.3390/app12010130>

23. Le, V., Keßler, A., & Folwaczny, M. (2023). Influence of DLP and SLA printer technology on the accuracy of surgical guides for implant dentistry in free-end situations. *International Journal of Computerized Dentistry*, 26(3), 217.

24. Morón-Conejo, B., Berrendero, S., Salido, M. P., Zarauz, C., & Pradíes, G. (2024). Accuracy of surgical guides manufactured with four different 3D printers. A comparative in vitro study. *Journal of Dentistry*, 148, 105226. <https://doi.org/10.1016/j.jdent.2024.105226>

25. Wu, D., Zhao, Z., Zhang, Q., Qi, H. J., & Fang, D. (2019). Mechanics of shape distortion of DLP 3D printed structures during UV post-curing. *Soft Matter*, 15(30), 6151–6159. <https://doi.org/10.1039/c9sm00725c>

26. Lo Russo, L., Guida, L., Zhurakivska, K., Troiano, G., Di Gioia, C., Ercoli, C., & Laino, L. (2023). Three dimensional printed surgical guides: Effect of time on dimensional stability. *Journal of Prosthodontics*, 32(5), 431–438. <https://doi.org/10.1111/jopr.13573>

27. Tahir, N., & Abduo, J. (2022). An in vitro evaluation of the effect of 3D printing orientation on the accuracy of implant surgical templates fabricated by desktop printer. *Journal of Prosthodontics*, 31(9), 791–798. <https://doi.org/10.1111/jopr.13485>

28. Rubayo, D. D., Phasuk, K., Vickery, J. M., Morton, D., & Lin, W.-S. (2021). Influences of build angle on the accuracy, printing time, and material consumption of additively manufactured surgical templates. *The Journal of Prosthetic Dentistry*, 126(5), 658–663. <https://doi.org/10.1016/j.jprostdent.2020.09.012>

29. Dalal, N., Ammoun, R., Abdulmajeed, A. A., Deeb, G. R., & Bencharit, S. (2020). Intaglio surface dimension and guide tube deviations of implant surgical guides influenced by printing layer

thickness and angulation setting. *Journal of Prosthodontics*, 29(2), 161–165. <https://doi.org/10.1111/jopr.13138>

30. Salazar Rios, A. L., Kesterke, M. J., Pylant, G. D., Barmak, A. B., Kontogiorgos, E. D., & Revilla-León, M. (2023). Effect of print orientation, storage conditions, and storage time on intaglio surface accuracy of implant surgical guides fabricated by using a stereolithography technology. *The Journal of Prosthetic Dentistry*. <https://doi.org/10.1016/j.prosdent.2023.08.016>

31. Keßler, A., Dosch, M., Reymus, M., & Folwaczny, M. (2022). Influence of 3D-printing method, resin material, and sterilization on the accuracy of virtually designed surgical implant guides. *The Journal of Prosthetic Dentistry*, 128(2), 196–204. <https://doi.org/10.1016/j.prosdent.2020.08.038>

32. Tahmaseb, A., Wu, V., Wismeijer, D., Coucke, W., & Evans, C. (2018). The accuracy of static computer-aided implant surgery: A systematic review and meta-analysis. *Clinical Oral Implants Research*, 29(S16), 416–435. <https://doi.org/10.1111/clr.13346>

33. Pessoa, R., Siqueira, R., Li, J., Saleh, I., Meneghetti, P., Bezerra, F., Wang, H., & Mendonça, G. (2022). The impact of surgical guide fixation and implant location on accuracy of static computer-assisted implant surgery. *Journal of Prosthodontics*, 31(2), 155–164. <https://doi.org/10.1111/jopr.13371>

34. Alkanderi, A. A. (2021). *Effect of printing layer thickness of implant surgical guides on the degree of deviation in the final implant position* (Master's thesis). The University of Texas School of Dentistry at Houston.

35. Panjnoush, M., Kheirandish, Y., Sharifi, R., & Mirjalili, F. (2023). Effect of slice thickness of 3D printer in fabrication of surgical guide on the accuracy of dental implant placement. *Journal of Oral Implantology*. <https://doi.org/10.1563/aaid-joi-d-21-00179>

36. D'haese, J., Van De Velde, T., Komiya, A., Hultin, M., & De Bruyn, H. (2012). Accuracy and complications using computer-designed stereolithographic surgical guides for oral rehabilitation by means of dental implants: A review of the literature. *Clinical Implant Dentistry and Related Research*, 14(3), 321–335. <https://doi.org/10.1111/j.1708-8208.2010.00275.x>

37. Burkhardt, F., Handermann, L., Rothlauf, S., Gintaute, A., Vach, K., Spies, B. C., & Lüchtenborg, J. (2024). Accuracy of additively manufactured and steam sterilized surgical guides by means of continuous liquid interface production, stereolithography, digital light processing, and

fused filament fabrication. *Journal of the Mechanical Behavior of Biomedical Materials*, 152, 106418. <https://doi.org/10.1016/j.jmbbm.2024.106418>

38. Piedra-Cascón, W., Krishnamurthy, V. R., Att, W., & Revilla-León, M. (2021). 3D printing parameters, supporting structures, slicing, and post-processing procedures of vat-polymerization additive manufacturing technologies: A narrative review. *Journal of Dentistry*, 109, 103630. <https://doi.org/10.1016/j.jdent.2021.103630>

39. Ide, Y., Nayar, S., Logan, H., Gallagher, B., & Wolfaardt, J. (2017). The effect of the angle of acuteness of additive manufactured models and the direction of printing on the dimensional fidelity: Clinical implications. *Odontology*, 105(1), 108–115. <https://doi.org/10.1007/s10266-016-0239-4>

40. Chen, Y.-W., Hanak, B. W., Yang, T.-C., Wilson, T. A., Hsia, J. M., Walsh, H. E., Shih, H.-C., & Nagatomo, K. J. (2021). Computer-assisted surgery in medical and dental applications. *Expert Review of Medical Devices*, 18(7), 669–696. <https://doi.org/10.1080/17434440.2021.1886075>

41. Vara, R., Lin, W., Low, J. K., Smith, D., Grimm, A., Calvert, G., Tadakamadla, S. K., Alifui-Segbaya, F., & Ahmed, K. E. (2023). Assessing the impact of resin type, post-processing technique, and arch location on the trueness and precision of 3d-printed full-arch implant surgical guides. *Applied Sciences*, 13(4), 2491. <https://doi.org/10.3390/app13042491>

42. Hüfner, M., David, S., Brunello, G., Kerberger, R., Rauch, N., Busch, C. V., Drescher, D., Bouraue, C., & Becker, K. (2024). Autoclaving-induced dimensional changes of three-dimensional printed surgical guides: An in vitro study. *Clinical Oral Implants Research*, 35(8), 821–829. <https://doi.org/10.1111/clr.14158>

43. Abduo, J., & Lau, D. (2020). Effect of manufacturing technique on the accuracy of surgical guides for static computer-aided implant surgery. *The International Journal of Oral & Maxillofacial Implants*, 35(5), 931–938. <https://doi.org/10.11607/jomi.8186>

44. Sharma, N., Cao, S., Msallem, B., Kunz, C., Brantner, P., Honigmann, P., & Thieringer, F. M. (2020). Effects of steam sterilization on 3D printed biocompatible resin materials for surgical guides—An accuracy assessment study. *Journal of Clinical Medicine*, 9(5), 1506. <https://doi.org/10.3390/jcm9051506>

45. Kessler, A., Reichl, F.-X., Folwaczny, M., & Högg, C. (2020). Monomer release from surgical guide resins manufactured with different 3D printing devices. *Dental Materials*, 36(11), 1486–1492. <https://doi.org/10.1016/j.dental.2020.09.002>

46. Wu, D., Huang, Y., Zhang, Q., Wang, P., Pei, Y., Zhao, Z., & Fang, D. (2022). Initiation of surface wrinkling during photopolymerization. *Journal of the Mechanics and Physics of Solids*, 162, 104838. <https://doi.org/10.1016/j.jmps.2022.104838>

47. Reymus, M., Lümkemann, N., & Stawarczyk, B. (2019). 3D-printed material for temporary restorations: Impact of print layer thickness and post-curing method on degree of conversion. *Int J Comput Dent*, 22(3), 231–237.

48. Al-Dulaijan, Y. A., Alsulaimi, L., Alotaibi, R., Alboainain, A., Akhtar, S., Khan, S. Q., Al-Ghamdi, M., & Gad, M. M. (2023). Effect of printing orientation and postcuring time on the flexural strength of 3D-printed resins. *Journal of Prosthodontics*, 32(S1), 45–52. <https://doi.org/10.1111/jopr.13572>

49. Kim, D., Shim, J.-S., Lee, D., Shin, S.-H., Nam, N.-E., Park, K.-H., Shim, J.-S., & Kim, J.-E. (2020). Effects of post-curing time on the mechanical and color properties of three-dimensional printed crown and bridge materials. *Polymers*, 12(11), 2762. <https://doi.org/10.3390/polym12112762>

50. Ntovas, P., Marchand, L., Basir, B., Kudara, Y., Revilla-Leon, M., & Att, W. (2025). Effect of storage conditions and time on the dimensional stability of 3d printed surgical guides: An in vitro study. *Clinical Oral Implants Research*, 36(1), 92–99. <https://doi.org/10.1111/clr.14362>

51. Taheri Otaghsara, S. S., Joda, T., & Thieringer, F. M. (2023). Accuracy of dental implant placement using static versus dynamic computer-assisted implant surgery: An in vitro study. *Journal of Dentistry*, 132, 104487. <https://doi.org/10.1016/j.jdent.2023.104487>

Abstract in Korean

임플란트 서지컬 가이드의 최적 안정성: 두께, 아치 형태 및 보관 기간의 영향

임플란트 수술에서 서지컬 가이드는 수술 정확성 향상에 기여하는 요소 중 하나이며, 그 구조적 안정성과 치수 정확성 확보가 매우 중요하다. 특히 수술 가이드의 형태, 두께, 보관 기간은 3D 프린팅 후 변형에 영향을 주며, 이는 임플란트 식립의 정밀도에 중대한 영향을 미칠 수 있다. 본 연구는 SLA 방식으로 제작된 tooth-supported 서지컬 가이드를 대상으로, 가이드 두께(2 mm, 3 mm, 4 mm), 아치 형태(partial arch, full arch), 보관 기간(0일, 1일, 3일, 7일, 14일)이 치수 안정성과 장착 정확도에 미치는 영향을 체계적으로 분석하였다.

총 48개의 가이드를 동일한 CAD 모델로 제작하고, 일정한 온도 및 습도 환경에서 보관한 후 정해진 시간 간격에 따라 스캐너로 측정하였다. 변형 정도는 RMSE(Root Mean Square Error)로 정량화 하였으며, 변형 분포는 color map 분석을 통해 시각적으로 평가하였다. 또한 각 가이드는 기준 모델에 장착하여 좌표 기반 장착 정확도 분석도 병행하였다.

RMSE 분석 결과, 대부분의 변형은 Day 0~1 사이의 초기 post-curing 단계에서 발생하였고, 이후 14일까지는 안정적인 치수 특성이 유지되었다. 특히 두께 3 mm 이상의 가이드는 보관 기간 동안 변형이 거의 발생하지 않았으며, full arch보다 partial arch에서 두께의 영향이 더 뚜렷하였다. 반면 partial arch의 2 mm 가이드는 Day 7에서 변형이 급격히 증가하는 경향을 보여, 얇은 구조가 외부 응력에 상대적으로 취약할 수 있음을 시사하였다.

Full arch 2 mm 가이드는 Day 1에서 최대 RMSE $100.65 \pm 10.31 \mu\text{m}$ 를 기록하였으며, partial arch 2 mm 가이드($70.89 \pm 5.61 \mu\text{m}$)보다 유의하게 높은 수치를 보였다. 전반적인 RMSE 범위에서도 full arch 그룹은 $96.35 \pm 13.07 \mu\text{m} \sim 100.65 \pm 10.31 \mu\text{m}$ 로, partial arch의 $70.89 \pm 5.61 \mu\text{m} \sim 75.39 \pm 9.17 \mu\text{m}$ 에 비해 구조적 불안정성이 더 큰 것으로 나타났다. 또한 4 mm 두께의 가이드는 모든 그룹에서 가장 낮은 변형 수치($69.33 \pm 9.76 \mu\text{m} \sim 73.38 \pm 11.15 \mu\text{m}$)를 유지하였다.

장착 정확도 분석에서도 두께 증가와 구조적 안정성은 밀접한 상관관계를 가지며, 3 mm 이상에서 가장 우수한 정합률을 보였다. 이러한 결과는 수술 가이드 제작 시 출력 직후 적절한 안정화 기간 확보와 함께, 최소 3 mm 이상의 두께를 유지하는 것이 변형 억제 및 임상 정확도 향상에 효과적임을 시사한다. 특히 partial arch 구조에서는 4 mm 이상의 두께를 확보하는 것이 바람직 할 수 있다.

핵심 되는 말 : 임플란트 수술 가이드; 가이드 두께; 치수 안정성; 아치 범위; 보관 기간; 장착 정확도; 평균 제곱근 오차; 3D 프린팅